An Analysis of fcMRI data in Schizophrenia

Hejazi, Nima
nhejazi

Lin, Feng
LiamFengLin

Zhao, Luyun
lynnzhao92

Zhou, Xinyue
z357412526

December 12, 2015

Abstract

We report analyses intended to explore the functional magnetic resonance imaging (fMRI) data collected in studies conducted by Repovs et al., on the manner in which brain network connectivity is related to schizophrenia [1, 2]. A host of exploratory analyses, combining both classical linear modeling methods and machine learning, were used in order to gain further insights into the fMRI data examined.

1   Introduction

The human central nervous system is a complex dynamic network, consisting of numerous functional regions that coordinate everything from simple reflexes to complicated thoughts. In an effort to better understand the manner in which functional changes contribute to the symptoms of schizophrenia, Repovs *et al.* conducted neuroimaging studies, including both functional connectivity magnetic resonance imaging (fcMRI) and diffusion tensor imaging (DTI), on many subjects, with their goal being to characterize the activity of several brain regions chosen *a priori*, and to develop an understanding of how the functional activities of these regions may differ across health states [1, 2].

1.1   Generalized Linearl Model

The goal of GLM with respect to our dataset is to detect the activation clusters of target and non-target events in one subject in the control (healthy) group. An activation cluster refers to a group of neighboring voxels activated beyond certain statistical thresholds (e.g., t-test, t-values) by defined events. We did not set up a quantifiable criterion – for example, to definitively separate one cluster from a neighboring cluster, but provide qualitative evidence in terms of coefficient and t-value maps. Please see the methods section that follows for the target and non-target events definitions.

GLM is performed for both 0-back and 2-back tasks for the subject so that we can assess the effect of different memory loads on activation clusters. Through the GLM, we are better able to access the noise structure of the data, so that we can remove the noise regressors as a step towards a connectivity analysis.

Besides analyses pertaining to the goals enumerated above, we performed various exploratory data analyses (EDA), such as K-Means clustering, correlations with different baseline functions that helped in understanding the data, and detection of root mean square (RMS) outliers, and more. The details of the EDA and relevant discussion of the results can be found in the appendix.

1.2   Connectivity Analysis

We are interested in the neural responses of the schizophrenic patients in a memory-related task, compared to the healthy controls. The goal of connectivity analysis is to compare the functional brain connectivity, measured by ROI-ROI correlations of 2-back task data between the four networks of the brain (DMN, FP, CO, CER), across controls (referred to as CON and composed of members of the control group and their siblings) and schizophrenics (referred to as SCZ and composed of patients with schizophrenia and their siblings). The task data was pre-precessed by removing the noise regressors after fitting the GLM described above. The four aforementioned networks are thought to be critical for cognitive function, as defined in the paper: (1) default mode network (DMN); (2) dorsal fronto-parietal

network (FP); (3) cingula-opercular network (CO); (4) cerebellar network (CER) [2]. We restrict our focus to the 2-back task because it is the most cognitively difficult to perform amongst the three levels of the n-back tasks and requires the highest memory load, thus making it more likely to reveal the differences of the response of the brains of the patients versus those of the controls.

2   Data

The analyses reported in this paper are based on data generated in a series of neuroimaging experiments conducted by Barch, Repovs, & Csernansky. The aim of these experiments was to ascertain the activity of several brain networks thought to be associated with depressed cognitive function in individuals with schizophrenia by collecting functional connectivity magnetic resonance imaging (fcMRI) data on healthy individuals, individuals with schizophrenia, and the (healthy) siblings of participants in either of the two former groups [2]. For the purposes of the analyses reported in this paper, the imaging data were acquired from the OpenfMRI project (`https://openfmri.org/`), where they are listed with accession number ds115. The data is available for groups of subjects, with each subject-specific data directory containing anatomical MR imaging data, functional MR imaging (using the BOLD contrast) data, and diffusion tensor imaging (DTI) data. In this preliminary report, the analyses are restricted to the BOLD functional MR imaging data, for 8 subjects among the pool of 102 subjects for which data are available, with most analyses (ranging from linear modeling to machine learning with K-Means) taking the form of exploratory examinations into the structure of this imaging data.

3   Methods

3.1   Data Preprocessing

Except for Extended RMS in EDA, the standard preprocessed BOLD images were used. They were already preprocessed with (1) motion correction (co-registration in time to partially correct for movement during the run and between runs); (2) temporary high-pass filtering to remove low frequency drifts and/or noise; and (3) registration to a standard anatomical template (the MNI template). In EDA, we detected several extended root-mean-square (RMS) outliers for the BOLD datasets. This further justified the need for temporary smoothing. For our preprocessing steps, first five images of each run were removed to allow measurements to achieve steady state. Each image was passed through a gaussian filter of $\sigma = 2$. This spatial smoothing approach assumes that fMRI data inherently show spatial correlations due to functional similarities of adjacent brain regions. To address the fact that boundary voxels of the brain were smoothed with measurements outside the brain, we implemented substitution of voxels near but outside the boundaries of brain with neighboring measurements within the boundary of the brain. However, this was not applied to connectivity portion of the analysis because the implementation was very slow and would take several hours on 20 subjects.

3.2   Data Analysis

3.2.1   Generalized Linear Model

Before proceeding to discussions of the specifics of our GLM approach, we believe it worthwhile to discuss the details of the condition files in the dataset because we make use of all condition files in the GLM. A major problem we encountered was that the keys in the metadata folder of the dataset that was provided does not correspond to the condition files, so the keys and the related descriptions of the condition files are redefined as given below.

- cond001: Start cues for both blocks of the run.
- cond002: The visual stimuli (i.e. letters) presenteed to the subject. The intensities are all one becasue there is only one homogeneous event type.
- cond003: The target and non-target events during the run. A target is the event that the current letter that is the same as the nth preceeding letter. Note that for 0-back, the 0th preceeding letter is pre-specified before the run instead of being presented continuously throughout the run. A non-target is the opposite of a target, in which the current letter is not the same.

- cond004: Done cues for both blocks of the run.

- cond005: Start and durations of the two blocks with a rest (i.e. fixation) period in between the blocks. This is different from resting-state data, which is mentioned in the reference papers but is not included on the OpenfMRI website.

- cond006: This is unknown and is not explained in the paper.

- cond007: Errors made by the subject when responding for each letter shown whether it was the same as a pre-specified (0-back) or preceding (1,2-back) letter.

We now proceed to describing the regressors in the GLM on each voxel time course. For all convolutions below, a specified condition on-off time course file was convolved at a time unit of 0.01 TR with a gamma function and take the convolved values at the start of each TR. After outlineing the regressors, one of the design matrix is shown as a figure below.

- reg001: Convolution of target events from cond003. Essentially, we split cond003 into separate regressors, target and non-target with the assumption that they different in the levels of activities.

- reg002: Convolution of non-target events from cond003.

- reg003: Convolution of error events from cond007.

- reg004: On-off time course from cond005. This regressor is included to account for mean differences in the two blocks of the same run.

- reg005: Convolution of start cues from cond001. This is separated from the target and non-target regressors in that it is not part of tasks and that it is not likely to involve heavy working memory load as tasks.

- reg006: Convolution of done cues from cond004. It has the same purpose as reg005.

- reg007 and reg008: A linear drift term and a quadratic drift term included as potential nuisansance regressors. Their significance is investigated below.

- reg009 and reg010: The first two principal components of the data. Based on the projections shown below, we decide that the first two are not functional features.
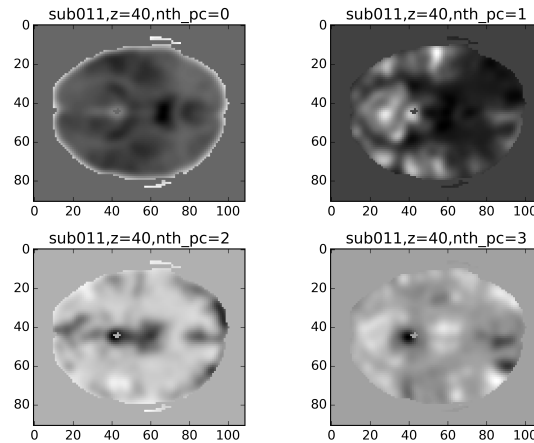
- reg011: Intercept term.

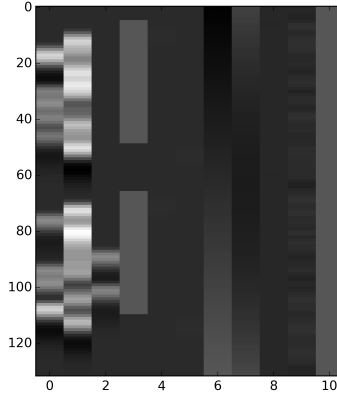Figure 1: The first four Principal Components (pc) for sub011, 0-back.

Figure 2: The design matrix for subject 011, 2-back. The indices correspond to the regressors from reg001 to reg011. Index 4 and 5 are almost unidentifiable from the graph because they are convolved from only a few single neural prediction values and hence are very small.

For each β on each voxel time course, a linear regression two-tailed t-test is conducted to access whether there is a significant linear relationship between the dependent variable Y and the regressor associated with the β, with significance levels of 0.05 for each test.

Null Hypothesis: $\beta = 0$

Alternative Hypothesis: $\beta \neq 0$

Instead of plotting out the regions of siginificant p-values, the t-value map of the entire brain is presented within the results section that follows.

Before performing t-tests, we assess the validity of t-tests by examining its assumptions. The two main assumptions are (1) the residuals of each linear model are independent and identically distributed (i.i.d), and (2) residuals for the model are normally distributed. The Shapiro-Wilk test is performed on the residuals of each voxel time course in the linear model. 37703 out of 207766 voxels fail this test; however, when performing a large number of statistical tests, some will have p-values less than 0.05 purely by chance (that is, it now becomes necessary to control the false discovery rate). To test the normality of several models together, three multiple comparison tests (namely, Bonferroni, Hochberg, and Benjamini-Hochberg), are performed, and results are shown below [1].

Bonferroni: normality assumption is violated in 6 voxels.

Hochberg: normality assumption is violated in 262 voxels.

Benjamini-Hochberg: all of voxels pass the normality test.

In summary, we can conclude that our assumption of normality in the residuals is generally valid.

3.2.2 Connectivity Analysis

The roadmap for the analytic steps followed to examine connectivity is as follows:

1. Removal of noise regressors from the voxel time series. Linear model as defined in the GLM section was fitted to each of the BOLD dataset. The residuals after removal of the noise regressors (i.e. reg003 to reg010 listed in the GLM section).

---

[1]The results were generated from our analysis scripts, and can be found in the results folder at *sub011_task003_linear_model_normality_test_failure_rates.csv*

2. Extraction of voxels per region of interest (ROI): ROIs of the four networks respectively are defined by a center and a diameter as 15mm [2]. Two validations are made before the analysis: (1) it is ensured that the ROIs are non-overlapping by setting the diameters for each ROI sphere as less than the minimum distance between any two given ROIs in the full set, and (2) ROIs are represented as spheres instead of cubes in order to better approximate the underlying neurobiology and to make easier the trouble associated with computing minimum distances between the ROIs in the set.

3. In order to compute the ROI-ROI correlations, several steps were taken: (1) for each ROI in a given network, the corresponding voxels were extracted and their time series were averaged to obtain a single average time series, (2) the ROI-ROI correlations between ROIs of each network-network pair were computed using the average time series, (3) for any two networks, which are composed with independent ROIs, we obtained the correlation matrix containing the correlation r-value of any two ROIs for the two networks, and (4) For each subject, we established the correlation matrix in (3) and group the r-values into two groups: CON and SCZ, according to the category of the subjects.

4. Unlike the paper, we decided to keep the original correlations to perform further analysis instead of taking Fisher's z transformation of the correlations. Fisher's z transformation is a function of correlation r aimed at constructing a statistic asymptotically normal so that a variety of analysis and tests, such as computing confidence intervals, can be performed. Two requirements need to be met for z to be approximately normal: 1) r is between variables from a bivariate normal distribution; 2) Sample size should be $n \geq 10$. Although some of the some samples shows a normal pattern based on the Gaussian quantil-quantile plot, many others have heavy-tailed density, violating the first requirement to arrive at a normal z value. Also, abnormally high z values were present in our results because Fisher's z transformation has asymptotic behavior at r close to ± 1, causing the analysis to be extremely inaccurate had we chosen to z-transform the r values.

3.2.3 Permutation Tests

To statistically confirm existing difference shown on the graph in the previous section, permutation test on correlation data has been performed. In this hypothesis testing, H_0: $r_{con} = r_{scz}$, H_i: $r_{con} \neq r_{scz}$. The method of implementing the permutation test under our framework was described below:

For each pair of networks i (namely, bFP-CO, bDMN-CER, bCO-CER, bDMN-CO, bFP-CERT, bDMN-FP),

- Calculate the difference between mean values of two groups:

$$diff^i = r_{con}^i - r_{scz}^i \tag{1}$$

- Create a data pool using two vector of correlations for different groups (r_{con}^i, r_{scz}^i). Permutation of the pool of data is applied, and treat first bunch of data in the vector to form a permutated r_{con}^i, saying, $r_{con}^i(p_k)$, and the data left is $r_{con}^i(p_k)$. Also notice that the length of vector in corresponding group should be kept. Take the difference between $r_{con}^i(p_k)$ and $r_{con}^i(p_k)$ and store the value as $diff^i(p_k)$ (k is the index of permutation). Repeat previous step for 50,000 times, creating a difference permutation vector.

  $pool_i = (r_{con}^i, r_{scz}^i)$ *i is different pair of networks.* $diff^i(p_k) = r_con^i(p_k) - r_scz^i(p_k) diff^i = (diff^i(p_1), diff^i(p_2), \ldots$

- Calulate the proportion of data less than $diff_i$ in the vector p, reject H_0 if p is less than $\alpha = 0.05$

4 Results

4.1 Linear Modeling

As the 0-back task serves primarily as an object recognition task with respect to the activation it induces in the central nervous system, it would be expected that visual processing centers of the brain would be found to be most activated. As seen in both the beta maps and the associated t-value maps, there is considerable (and significant) activation of occipital cortex as well as various regions of the frontal cortex. In contrast to the responses observed with respect to the 2-back task presented below, the coefficient
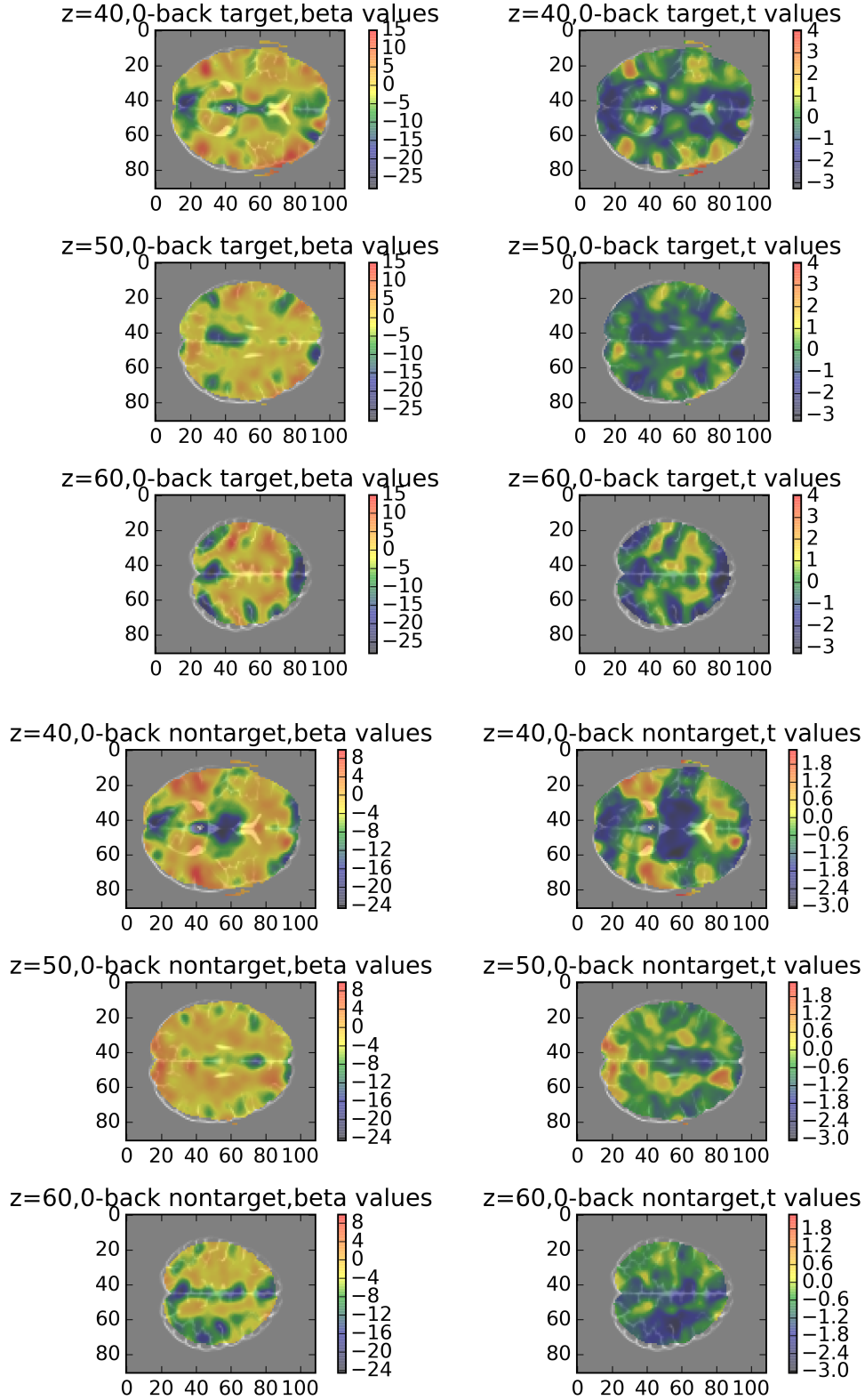
Figure 3: Above: 0-back target beta values and t values from two-tailed t tests against the null hypothesis of $\beta = 0$; Below: non-target beta values and t values from two-tailed t tests against the null hypothesis of $\beta = 0$. Both are based on linear model for sub011 / 0-back, as discussed in the method section. The colors are plotted on the same scale for graphs in the same column.

maps for the 0-back task for target images indicates fair amounts of activity across many regions of the brain, as would be expected of a general recognition test, whereas, in the 2-back task for target images, there is noticeably increased magnitudes in the activation of regions in the occipital cortex and in the frontal lobes, as would be expected of a task that involves working memory. It is worth noting that there is considerably less difference between the 0-back target vs. non-target activation patterns than between the 2-back target vs. non-target activation patterns, agreeing with the expectations based on psychological constructs such as working memory.

The two figures above display the observed activation patterns present in the 2-back task, which would be expected to activate regions of the prefrontal cortex more significantly than the 0-back task, on the basis that subjects must hold specific representations in memory in order to successfully complete this task. Furthermore, differences in the activation patterns between the target and non-target 2-back tests shows that the activation during the target task is less distributed, activating more specific regions, as opposed to the generalized activity created by undergoing the non-target 2-back task.

The non-target 2-back task activation patterns and associated t-value maps for the coefficients estimated from the linear model indicate that the non-target task generates activity across many regions of the central nervous system, in particular subregions in the frontal lobes (as seen in slice z=60) as well as numerous occipital and midbrain region activations (as seen in the slices z=50 and z=40). The many regions activated in the non-target 2-back analyses contrast sharply with the 2-back activations in the target group, as activations induced in the slices shown for that category are noticeably more focused in the occipital and frontal lobes.

The t-values associated with the coefficient estimates of the activation patterns in the 2-back target task show rather significant activation of frontal and midbrain regions, with these neural activations matching the more focused activation expected of a task more associated with inducing higher cognitive load. What is more, the differences in activation displayed by the two horizontal slices shown above illustrates how activation is distributed across the depths of the whole brain, in general activating frontal lobe regions associated with cognitive activity as well as occipital regions associated with visual task performance. With respect to the non-target activation patterns displayed in the slices shown below, the map of t-values indicate that activation is much more generally distributed across the brain in the non-target 2-back task, as would be expected of an error-based neural process.
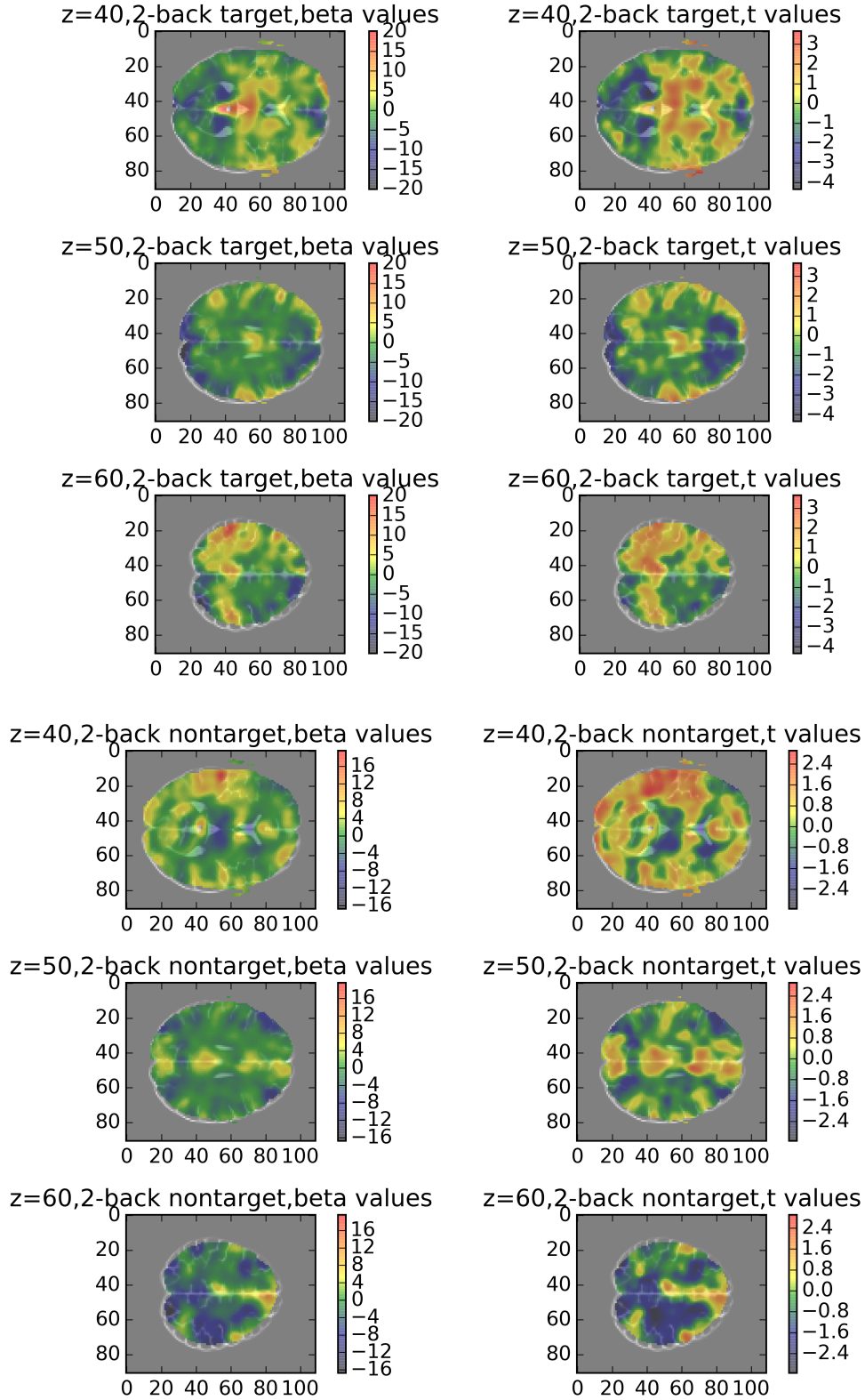
Figure 4: Above: 2-back target beta values and t values from two-tailed t tests against the null hypothesis of $\beta = 0$; Below: non-target beta values and t values from two-tailed t tests against the null hypothesis of $\beta = 0$. Both are based on linear model for sub011 / 2-back, as discussed in the method section.
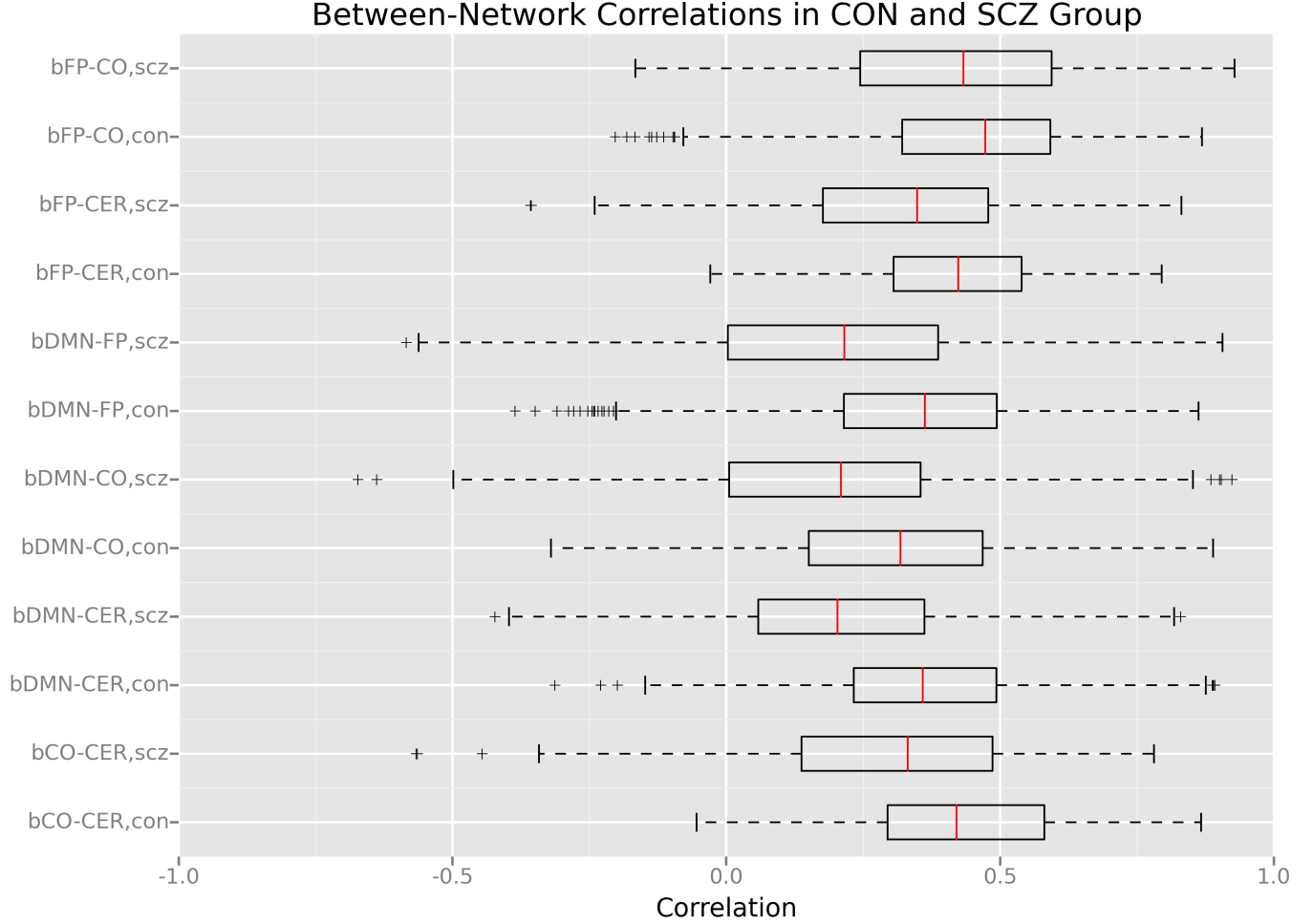
4.2 Connectivity Analysis

Figure 5: The connectivity plot comparing schizophrenics (SCZ) and controls (CON) between networks. For visual comparison, the CON group and SCZ group are interleaved in order to show results for the same network-nework pair side by side.

We performed the analysis on 20 subjects, including 12 SCZ (6 schizophrenias and 6 schizophrenia siblings) and 8 CON (4 controls and 4 control siblings). As shown in the figure above, the individuals with schizophrenia and their siblings (SCZ) showed an overall reduction in connectivity between the cognitive control networks as compared to CON, as indicated in the box plots of the correlations between networks for CON and SCZ. Previous studies concluded that there is reduced distal connectivity for individuals with schizophrenia, especially between the FP and CER networks and the CO and CER networks [1, 2]. However, the two results are not comparable in the following ways: (1) we use a smaller dataset of 20 subjects versus 102 subjects used in the reference paper, and (2) in the reference papers, many more nuisance regressors were removed from the BOLD time series. We only removed a few common noise regressors outlined in the methods section above. We obtained results similar to the previous work and provided similar evidence that schizophrenia reflects a disconnection syndrome. We also performed the permutation test in different pairs of networks, and found all of the test had rejected the null hypothesis. Therefore, we can conclude that the mean value of CON groups are significantly less than that of SCZ

group. [2]

Within-network correlations are not within the scope of our analysis, but a graph showing the results for within-network correlations is included in the appendix.

5 Discussion

References

[1] G. Repovs et al., *Brain network connectivity in individuals with schizophrenia and their siblings*, Biological Psychiatry, 69 (2011), pp. 967–973.

[2] ———, *Working memory related brain network connectivity in individuals with schizophrenia and their siblings*, Frontiers in Human Neuroscience, 6 (2012), pp. 1–15.

---

[2]The results were generated from our analysis scripts, and can be found in the results folder at *connectivity_permutation_result.csv*

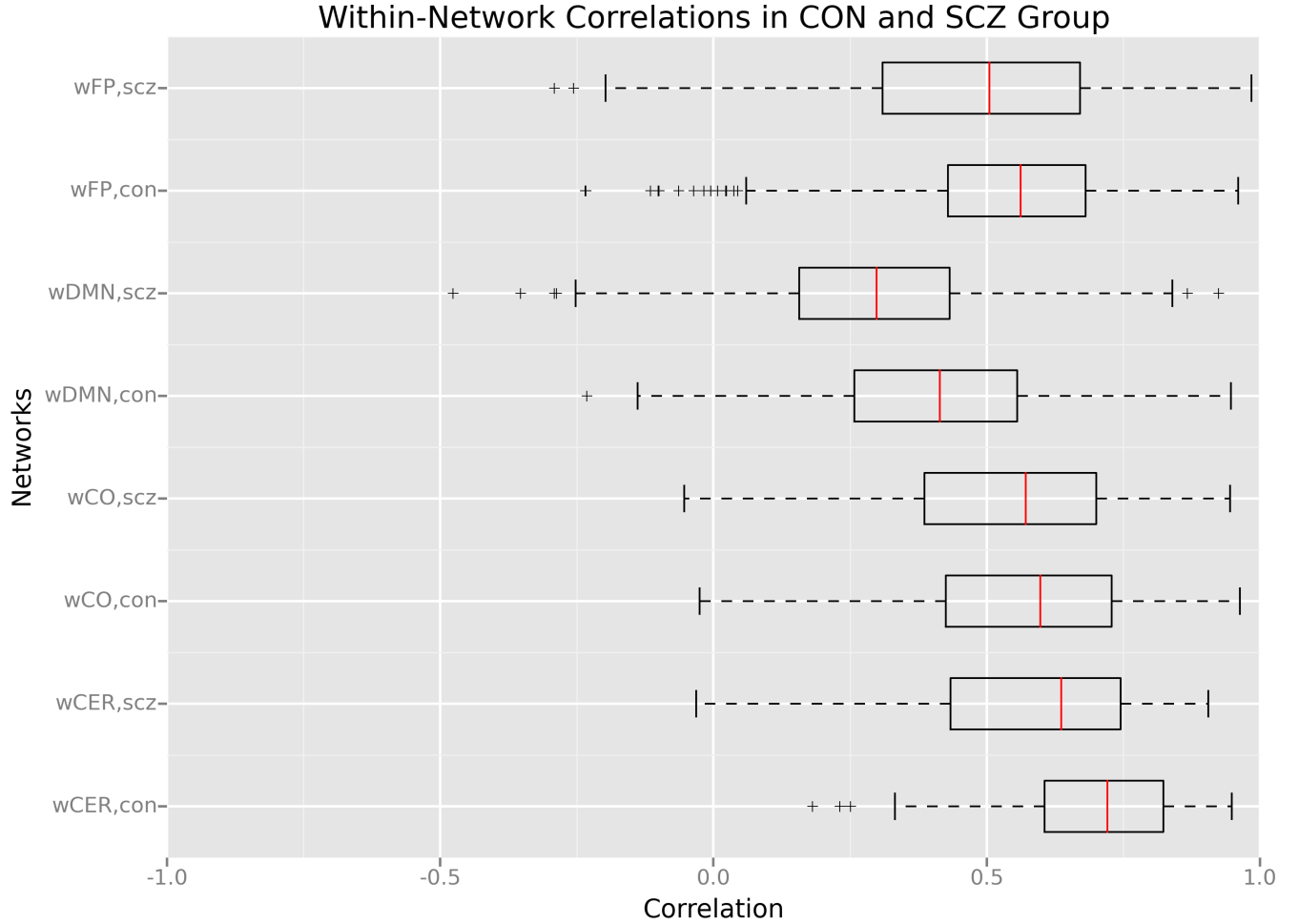# A   APPENDIX I - Results for Within-Network Correlations

Figure 6: The connectivity plot comparing schizophrenics (SCZ) and controls (CON) within networks. For visual comparison, the CON group and SCZ group are interleaved in order to show results for the same network side by side.

B   APPENDIX II - Exploratory Data Analysis

B.1   Data Fetching and Preprocessing

For all BOLD datasets, we removed the first five images to allow signals to achieve steady state. In addition, we prepared scripts to detect the root mean square (RMS) difference outliers using the inter-quartile range (IQR) to define outliers. This was done because these images could contain a sudden widespread shift in signals caused by hardware issues.
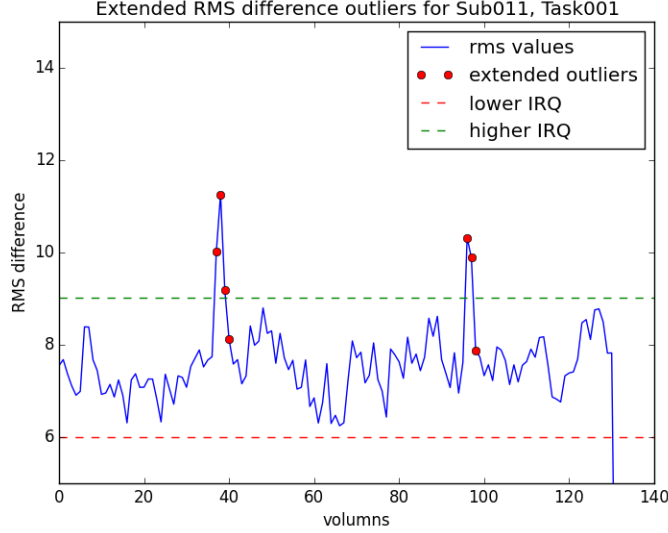
Figure 7: The extended RMS outliers for the BOLD images for sub011, 0-back

Some preprocessing tasks are analysis-specific. As will be discussed in a later section, we scaled BOLD signals per time step to use them as one of the feature sets for k-means clustering.

B.2 Correlations with Baseline Functions

This set of methods aimed to produce an image identifying the regions which showed significant signal change in response to the task. The analysis was done by calculating correlation coefficients (r) between the bold signal along the time course and a reference waveform, for each voxel. The reference waveform was extracted from a condition file. Condition file 003 was chosen because while it did not contain all stimuli presented to the subject, such as start and done cues, it included all target and non-target events and this thought to be sufficient to elicit functional differences of the brain during the run. A high value of the correlation coefficient indicated that fluctuation of the signal in the locale of the brain was task-dependent, hence activated by the task.

For a bold signal X, and a reference waveform Y, the correlation coefficient is calculated as below.

$$r = \frac{\Sigma_{i=1}^{n}(X - \bar{X})(Y - \bar{Y})}{\sqrt{\Sigma_{i=1}^{n}(X - \bar{X})^2 \Sigma_{i=1}^{n}(Y - \bar{Y})^2}} \tag{2}$$

The two methods were differentiated by two types of reference waveforms: (1) square wave using on-off neural prediction from condition file (SW method), and (2) a convolved function on neural predictions with a gamma haemodynamic response function (HRF) (CF method).

Here, the two types of analysis were compared. By comparing the activated regions under square wave time course (left) and convolved time course (right), we could see that compared to SW method, the CR method gives more reasonable and detailed results.
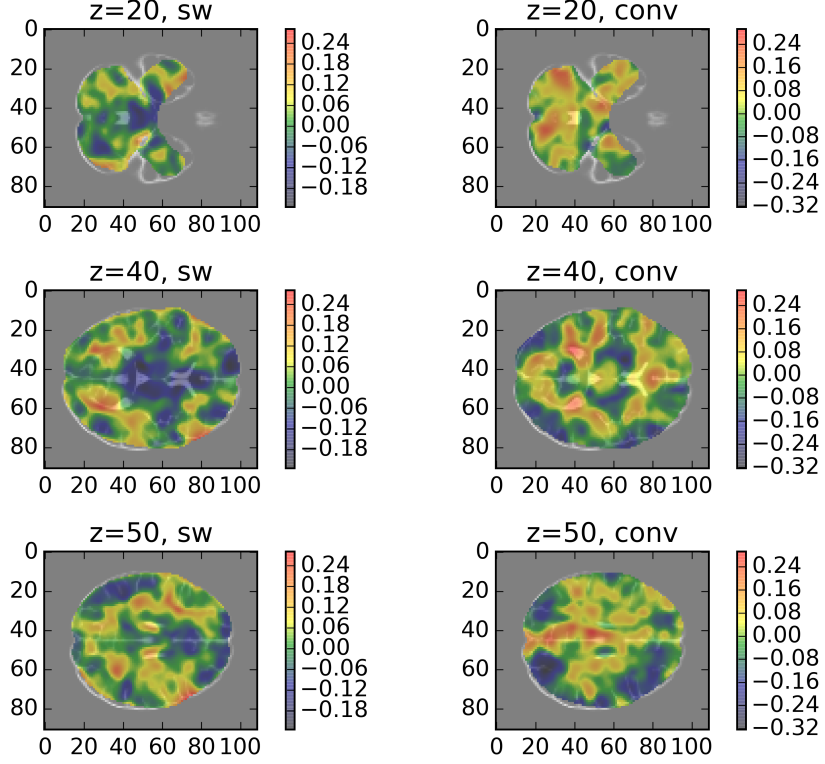
Figure 8: Voxel-wise correlations for square-wave and gamma baseline functions, sub011, 0-back, cond003.

B.3 Clustering with K-Means

K-means clustering is an unsupervised technique which aims to partition n observations into k clusters based on a feature set of n features. Each observation is classified into the cluster with the nearest mean. In our case,k was chosen to be 6. Input to k-means clustering followed the same treatment as discussed in the Linear Model section of the paper. Standard fMRI data was and the first two Principal Components were removed following the analysis in the Linear Model section of the paper. After that, it was spatially smoothed with gaussian kernel of $sigma = 2$. The rationale of removing the first two Principal Components was to remove differences caused by anatomical or other noise features as much as possible, in the hope that k-means can cluster the brain to functional regions.

We did not involve the condition files in the clustering. This was because during the same run, the time courses in the same region of the brain were subjected to the same functional influences. Hence, k-means should be able to detect differences in patterns of the time courses between regions.
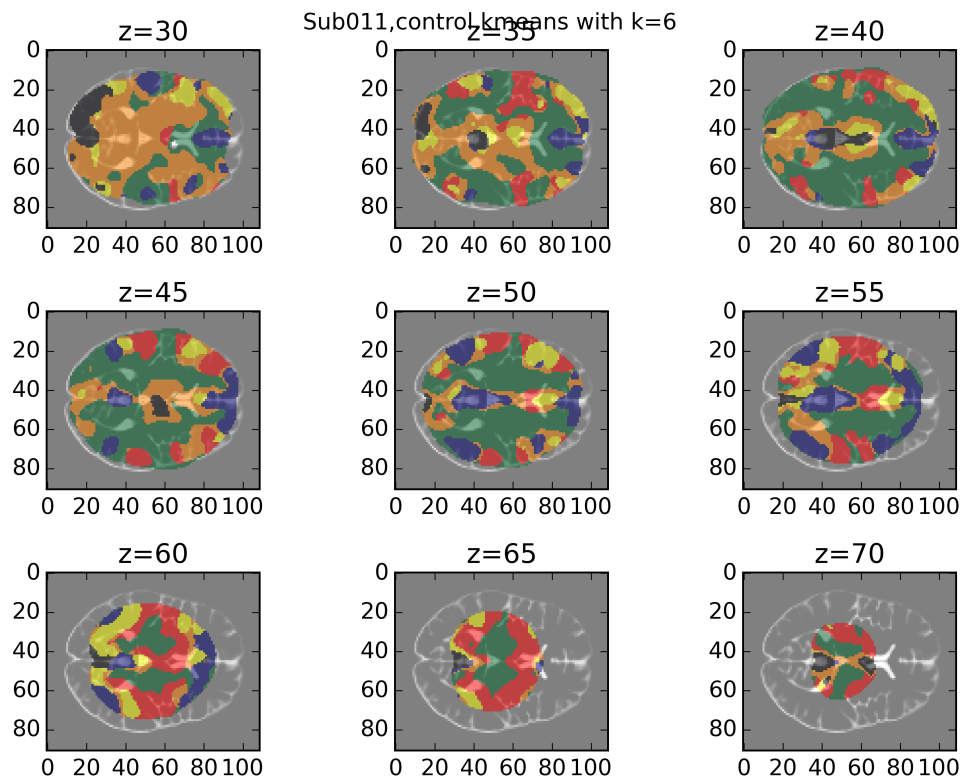
Figure 9: K-means result for $k = 6$ on smoothed standard fMRI data after removal of first two Principal Components, sub011, 0-back.